Communications on Applied Nonlinear Analysis
ISSN: 1074-133X
Vol 32 No. 3 (2025)

Some Reverse Topological Indices of Comet and Double Comet Graphs

John Rafael M. Antalan[1]*, Richard P. Tagle[2]
[1]Department of Mathematics and Physics, College of Science Central Luzon State University
[2]Science City of Muñoz, Nueva Ecija, 3120, Philippines
jrantalan@clsu.edu.ph

Article History:

Received: *22-07-2024*

Revised: *10-09-2024*

Accepted: *29-09-2024*

Abstract

Introduction: Chemical Graph Theory or CGT for short, is a transdisciplinary field of Mathematics wherein graphs are used to represent chemical compounds. Under this representation, the atoms of a chemical compound are expressed as vertices, while the bonds connecting these atoms are expressed as edges. Once the graph representation of a chemical compound has been determined, graph-theoretic techniques can now be used to determine various topological indices associated with the chemical compound. Topological indices are invariants of a graph that have predictive power for the chemical properties of a chemical compound. In CGT, trees, being connected and acyclic, have been an essential class of graphs. This is because, most compounds have acyclic molecular structures. In the 2023 study by Gowtham and Husin, various reverse topological indices of a family of trees called bistar graphs have been determined.

Objectives: Motivated by the work of Gowtham and Husin, we determine some reverse topological indices of another family of trees called comets and double comets. Double comets are natural extension of bistar graphs. We also give a certain computational application of our results on double comet graphs. Finally, we investigate the relationship between the reverse topological indices of bistar graphs and double comets.

Methods: Several important graph-theoretic concepts were used to analyze some important properties of comets and double comets, leading to the computation of their reverse vertex degree based topological indices.

Results: The following reverse vertex degree-based topological indices for comets and double comets were determined: Reverse sum-connectivity, First reverse Zagreb, Second reverse Zagreb, Reverse arithmetic-geometric, Reverse geometric-arithmetic, Reverse Sombor, and Reverse Nirmala. A computational application of the results to a certain chemical compound (2,2,4,4-Tetramethylpentane) or C_9H_{20} were also demonstrated.

Conclusions: The results of the paper provided an extension to an existing result on the reverse vertex degree-based topological indices of bistar graphs by considering double comet graphs. Several topological reverse vertex degree-based topological indices were also computed for comet graphs. The computed topological indices were also applied in determining some invariants of a certain chemical compound. For future studies, we recommend that reverse vertex degree based topological indices of other family of trees will be considered.

Keywords: molecular graph, topological index, reverse vertex degree, comet, double comet

AMS Classification Numbers: 05C05, 05C07, 05C09

1. Introduction

In this paper, the graphs that we will consider are all simple, connected, and finite. Also, throughout this paper, we follow the common notation $V(G)$ and $E(G)$ for the vertex set and edge set of a graph G, respectively. We also have adapted the graph theory notations used by Wagner and Wang in [27], and refer to the same text, for any reader who needs to recall some graph-theoretic concepts that were mentioned, but not explicitly discussed in detail in this paper.

In CGT, the atoms of a chemical compound and the bonds connecting them are expressed respectively as vertices and edges of a graph, thereby obtaining its molecular graph. Under this representation, the vertices corresponding to hydrogen atoms are usually removed since the valency or degree of Hydrogen is one. For example, the ball and stick chemical structure of 2,2,4,4-Tetramethylpentane (C_9H_{20}) in Figure 1a has a corresponding molecular graph shown in Figure 1b.

Figure 1: (a)The ball and stick structure of 2,2,4,4-Tetramethylpentane C_9H_{20} taken from PubChem [1]. (b) The molecular graph of 2,2,4,4-Tetramethylpentane.

Once the molecular graph of a chemical compound has been obtained, one can now use graph theoretic concepts and techniques to determine various topological indices associated with the compound. A topological index is a computed numerical value associated with the molecular graph that has predictive power for the chemical properties of the chemical compound.

Topological indices may be classified according to the graph property in which they are defined. It is said to be distance-based, if it is derived based on the concept of distance between each pair of vertices in the graph. On the other hand, a topological index is vertex degree-based, if it is defined based on the degree of the vertices in the graph.

One popular topological index based on distance is the Wiener index denoted by $W(\cdot)$. For a graph G, its Wiener index is defined as

$$“W(G) = \sum_{\{u,v\}\subseteq V(G)} d(u,v)”,$$

wherein the notation $d(u,v)$ refers to the distance between the vertices u and v in G. This index was named after Harry Wiener, a chemist who proposed this concept in 1947 [29]. Since the publication of this work by Wiener, various studies related to this index have been conducted with the recent works provided in [4, 5, 7, 6, 8, 9, 11, 20, 21, 31].

An example of a topological index based on vertex degree is the Randic index and its generalization denoted by $R(\cdot)$ and $R_\alpha(\cdot)$ respectively, where $\alpha \neq 0$. If G is a graph, then its generalized Randic index is given by

$$“R_\alpha(G) = \sum_{uv\in E(G)} [deg_G(u)deg_G(v)]^\alpha”,$$

wherein $deg_G(u)$ and $deg_G(v)$ refers to the degrees of vertices u and v in G respectively. For $\alpha = -\frac{1}{2}$, we have the "Randic index" while for $\alpha = 1$, we have the "second Zagreb index". The Randic index was named after Milan Randic who proposed the index in [25] in the year 1975. The second Zagreb index, on the other hand, was introduced by Ivan Gutman and Nenad Trinajstic in 1972 and first appeared in [13]. These two vertex degree-based indices have been constantly considered as a topic of study, and are being used in the Quantitative Structure-Property Relationships (QSPR) modeling. Some recent use of Randic and the second Zagreb index and their variations for QSPR modeling can be shown in [3, 14, 15, 16, 17, 23, 24, 30, 33, 35].

In this study however, we will consider another type of topological indices which are dependent on the "reverse vertex-degree" of a vertex in a graph. Suppose G is a graph with maximum vertex degree $\Delta(G)$. For any vertex u in G, its reverse vertex degree, denoted by r_u is the quantity $\Delta(G)-deg_G(u)+1$, that is,

$$\text{"}r_u = \Delta(G) - deg_G(u)+1\text{".}$$

This concept was introduced by Kulli in 2018, where he computed the reverse Zagreb and reverse hyper-Zagreb index of rhombus silicate networks [18]. Since then, various research works on the determination of these types of indices for graphs and chemical materials have been conducted. These works can be viewed in [2, 19, 22, 26, 28, 32, 34, 36] and were discussed by Gowtham and Husin in their recent research article [12], which is the motivational work for this research study. Gowtham and Husin computed some reverse vertex-degree-based topological indices of bistar graphs which is an example of a tree [12]. Trees, being connected and acyclic, have been an essential class of graphs in CGT. For this study, we will determine some reverse vertex degree-based topological indices of other families of trees called comets and double comets.

2. Preliminary Concepts and Results

We will briefly discuss the recent research work of Gowtham and Husin regarding some reverse vertex degree-based topological indices of bistar graphs [12]. Moreover, essential preliminary results on comets and double comets will also be discussed which will be used in the results section.

2.1 Gowtham and Husin's Results for Bistar Graphs

A vertex $u \in V(G)$ is said to be a leaf if $deg_G(u) = 1$. A star of order n+1, denote by $K_{1,n}$ is a tree with n number of leaves and a central vertex of degree n. Presented in Figure 2 are the stars $K_{1,n}$ and $K_{1,m}$ respectively.

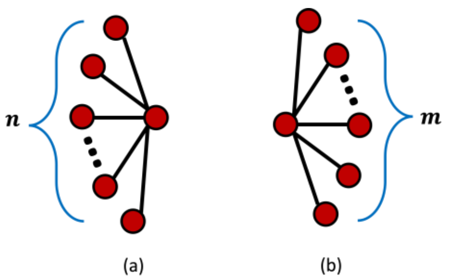

Figure 2: (a) The star $K_{1,n}$. (b) The star $K_{1,m}$.

The bistar graph denoted by $B(n;m)$ is a graph obtained by connecting the centers of two star graphs with n and m number of leaves respectively by an edge. The graph $B(n;m)$ is depicted in Figure 3.

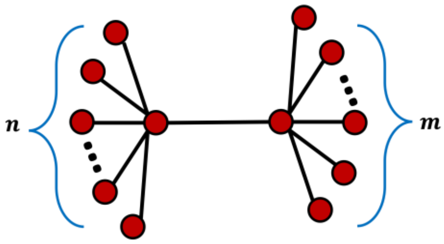

Figure 3: The bistar graph $B(n;m)$.

Gowtham and Husin calculated the following reverse vertex degree-based topological indices of $B(n;m)$: Reverse sum-connectivity ($RSCI(\cdot)$), First reverse Zagreb ($RM_1(\cdot)$), Second reverse Zagreb ($RM_2(\cdot)$), Reverse arithmetic-geometric ($RAG(\cdot)$), Reverse geometric-arithmetic ($RGA(\cdot)$), Reverse Sombor ($RSO(\cdot)$), and Reverse Nirmala ($RN(\cdot)$) in [12]. Their results are summarized in the table below. To eliminate cases, we introduce the notations $M = \max\{m,n\}$ and $\mu = \min\{m,n\}$.

Topological Index	Definition	Result for $B(n;m)$
$RSCI(\cdot)$	"$\sum_{uv\in E(G)} \frac{1}{\sqrt{r_u+r_v}}$"	$\frac{M}{\sqrt{M+2}}+\frac{1}{\sqrt{M-\mu+2}}+\frac{\mu}{\sqrt{2M-\mu+2}}$
$RM_1(\cdot)$	"$\sum_{u\in V(G)} r_u^2$"	$(M+\mu)(M+1)^2+(M-\mu+1)^2+1$
$RM_2(\cdot)$	"$\sum_{uv\in E(G)} (r_u\cdot r_v)$"	$\mu(M+1)+(M-\mu+1)(M\mu+\mu+1)$
$RAG(\cdot)$	"$\sum_{uv\in E(G)} \frac{r_u+r_v}{2\sqrt{r_u\cdot r_v}}$"	$\frac{M(M+2)}{2\sqrt{M+1}}+\frac{M-\mu+2}{2\sqrt{M-\mu+1}}+\frac{\mu(2M-\mu+2)}{2\sqrt{(M+1)(M-\mu+1)}}$
$RGA(\cdot)$	"$\sum_{uv\in E(G)} \frac{2\sqrt{r_u\cdot r_v}}{r_u+r_v}$"	$\frac{2M\sqrt{M+1}}{M+2}+\frac{2\sqrt{M-\mu+1}}{M-\mu+2}+\frac{2\mu\sqrt{(M+1)(M-\mu+1)}}{2M-\mu+2}$
$RSO(\cdot)$	"$\sum_{uv\in E(G)} \sqrt{r_u^2+r_v^2}$"	$M\sqrt{(M+1)^2+1}+\sqrt{(M-\mu+1)^2+1}+\mu\sqrt{(M-\mu+1)^2+(M+1)^2}$
$RN(\cdot)$	"$\sum_{uv\in E(G)} \sqrt{r_u+r_v}$"	$M\sqrt{M+2}+\sqrt{M-\mu+2}+\mu\sqrt{2M-\mu+2}$

Table 1: Various reverse degree-based topological indices of $B(n;m)$ obtained by Gowtham and Husin.

Motivated by the above results from Gowtham and Husin, we determine the same set of topological indices for comets and double comets in this paper.

2.2. Reverse Vertex Degree of Vertices of Comets and Double Comets

As mentioned in the previous subsection, this paper will investigate several reverse vertex degree-based topological indices of comets and double comets. In this subsection, we will discuss essential preliminary results on comets and double comets which are needed for the discussion of main results.

We begin by providing the definition of a path. A path with n number of vertices, denoted by P_n is the unique tree with only two leaves. The non-leaf vertices of a path are called internal vertices. In general, internal vertices are vertices of degree ≥ 2. The path P_4 with leaf vertices v_1 and v_4 and internal vertices v_2 and v_3 is presented in Figure 4.

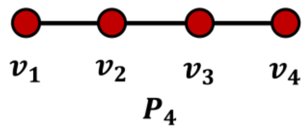

Figure 4: The path P_4 with v_1, v_4 as leaves and v_2, v_3 as internal vertices.

We are now at the position to define comet graphs. The comet $C_{m,n}$ is the tree obtained from path P_m by appending $n > 1$ edges to one end of P_m. The end vertex of P_m appended by n number of edges is called the branching vertex of $C_{m,n}$. In general, a branching vertex is a vertex of degree ≥ 3. We remark that the notation we used in denoting comet graphs, and later for double comets are the one used by Dogan Durgun and Toprakkaya in [10]. The comet $C_{4,5}$ with branching vertex v_b is depicted in Figure 5a while the comet $C_{m,n}$ is depicted in Figure 5b.

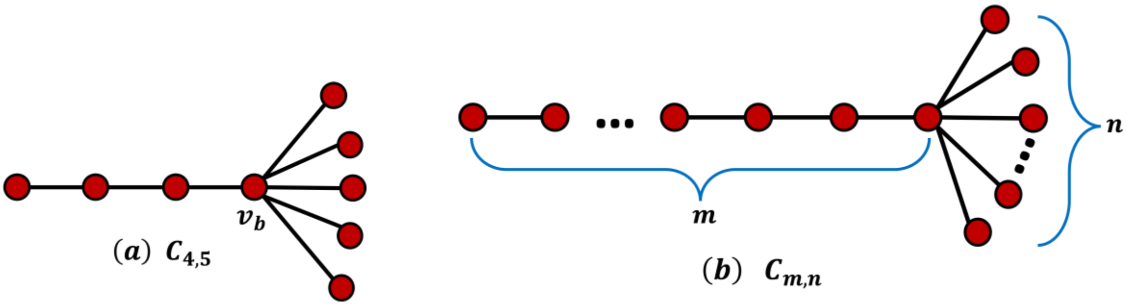

Figure 5: (a) The comet $C_{4,5}$ with branching vertex v_b. (b) The comet $C_{m,n}$.

On the other hand, the double comet $DC(m,m_1,m_2)$ is the tree obtained from path P_m by appending $m_1 > 1$ edges to one end of P_m and $m_2 > 1$ edges on the other end of P_m. In this case, the ends of P_m are the branching vertices of $DC(m,m_1,m_2)$. The double comet $DC(4,3,5)$ is shown in Figure 6a, while the double comet $DC(m,m_1,m_2)$ is depicted in Figure 6b.

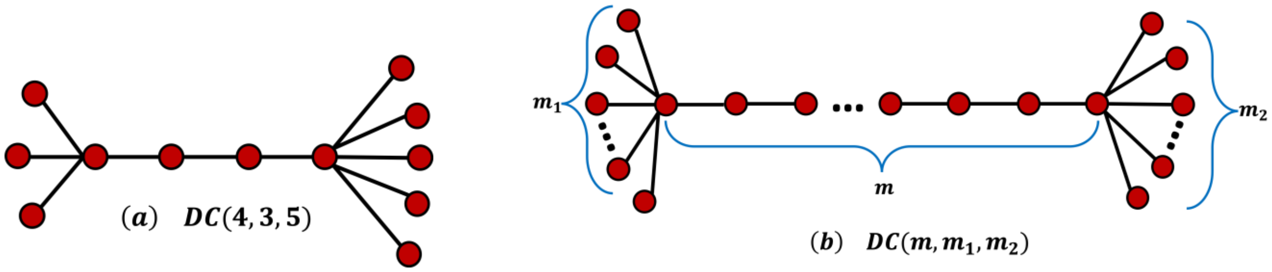

Figure 6: (a) The double comet $DC(4,3,5)$. (b) The double comet $DC(m,m_1,m_2)$.

Remark 2.1. *Before we continue, we remark that although based on definition, a branching vertex is an internal vertex, we reserve the term "internal vertex" for vertices that are internal but not branching in this paper.*

Now that we have already discussed the comet and double comet graphs, we are now ready to present results concerning the reverse vertex degree of their vertices.

Proposition 2.2. *If u is a vertex in $V(C_{m,n})$ then*

$$r_u = \begin{cases} n+1 & \text{if } u \text{ is a leaf} \\ n & \text{if } u \text{ is an internal vertex} \\ 1 & \text{if } u \text{ is a branching vertex} \end{cases} \quad (1)$$

Proof. We begin by noting that for $G = C_{m,n}$, we have $\Delta(G) = n+1$. Let $u \in V(G)$. Since u is a vertex in $V(G)$, then u is either a leaf with $deg_G(u) = 1$, an internal vertex with $deg_G(u) = 2$, or a branching vertex with $deg_G(u) = n+1$. If u is a leaf, then $r_u = \Delta(G) - deg_G(u) + 1 = (n+1) - 1 + 1 = n+1$. If u is an internal vertex, then $r_u = \Delta(G) - deg_G(u) + 1 = (n+1) - 2 + 1 = n$. Finally, if u is a branching vertex, then $r_u = \Delta(G) - deg_G(u) + 1 = (n+1) - (n+1) + 1 = 1$. This proves Proposition 2.2. □

We now end the section by stating and proving the next proposition.

Proposition 2.3. *Let* $M = max\{m_1,m_2\}$ *and* $\mu = min\{m_1,m_2\}$. *If u is a vertex in* $V(DC(m,m_1,m_2))$ *then*

$$r_u = \begin{cases} M+1 & \text{if } u \text{ is a leaf} \\ M & \text{if } u \text{ is an internal vertex} \\ M-\mu+1 & \text{if } u \text{ is a branching vertex with } deg(u) = \mu+1 \\ 1 & \text{if } u \text{ is a branching vertex with } deg(u) = M+1 \end{cases} \quad (2)$$

Proof. We begin by noting that for $G = DC(m,m_1,m_2)$, we have $\Delta(G) = M + 1$. Let $u \in V(G)$. Since u is a vertex in $V(G)$, then u is either a leaf with $deg_G(u) = 1$, an internal vertex with $deg_G(u) = 2$, a branching vertex with $deg_G(u) = \mu + 1$, and a branching vertex with $deg_G(u) = M + 1$. If u is a leaf, then $r_u = \Delta(G) - deg_G(u) + 1 = (M+1) - 1 + 1 = M + 1$. If u is an internal vertex, then $r_u = \Delta(G) - deg_G(u) + 1 = (M + 1) - 2 + 1 = M$. If u is a branching vertex with $deg_G(u) = \mu + 1$, then $r_u = \Delta(G) - deg_G(u) + 1 = (M + 1) - (\mu + 1) + 1 = M - \mu + 1$. Finally, if u is a branching vertex with $deg_G(u) = M + 1$, then $r_u = \Delta(G) - deg_G(u) + 1 = (M + 1) - (M + 1) + 1 = 1$. This proves Proposition 2.3. □

3. Several Reverse Vertex Degree Indices of Comets and Double Comets

3.1. Results for Comet Graphs

We now present our results for comet graphs. Throughout this subsection, we denote the comet graph $C_{m,n}$ by G.

Theorem 3.1. *Let* $G = C_{m,n}$. *The "reverse sum-connectivity index" of G denoted by* $RSCI(G)$ *is given by*

$$RSCI(G) = \frac{1}{\sqrt{2n+1}} + \frac{m-3}{\sqrt{2n}} + \frac{1}{\sqrt{n+1}} + \frac{n}{\sqrt{n+2}}.$$

Proof. We start by noting that the graph $G = C_{m,n}$ has $m - 1 + n$ edges with the following classification based on their end vertices: 1 leaf-internal edge, $m - 3$ internal-internal edges, 1 internal-branching edge, and n branching-internal edges. Combining these information with equation (1) in Proposition 2.2 and the definition of the reverse sum-connectivity index, we arrive at

$$\begin{aligned} RSCI(G) &= \sum_{uv \in E(G)} \frac{1}{\sqrt{r_u + r_v}} \\ &= \frac{1}{\sqrt{(n+1)+n}} + \frac{m-3}{\sqrt{n+n}} + \frac{1}{\sqrt{n+1}} + \frac{n}{\sqrt{1+(n+1)}} \\ &= \frac{1}{\sqrt{2n+1}} + \frac{m-3}{\sqrt{2n}} + \frac{1}{\sqrt{n+1}} + \frac{n}{\sqrt{n+2}}. \end{aligned}$$

□

Theorem 3.2. *Let* $G = C_{m,n}$. *The "first reverse Zagreb index" of G denoted by* $RM_1(G)$ *is given by*

$$RM_1(G) = (n + 1)^3 + mn^2 - 2n^2 + 1.$$

Proof. We start by noting that the graph $G = C_{m,n}$ has $m + n$ vertices with the following classification: $n+1$ leaf vertices, $m - 2$ internal vertices, and 1 branching vertex. Combining these information with equation (1) in Proposition 2.2 and the definition of the first reverse Zagreb index, we arrive at

$$\begin{aligned} RM_1(G) &= \sum_{u \in V(G)} r_u^2 \\ &= (n+1)(n+1)^2 + (m-2)n^2 + 1(1^2) \\ &= (n+1)^3 + mn^2 - 2n^2 + 1. \end{aligned}$$

□

Theorem 3.3. *Let* $G = C_{m,n}$. *The "second reverse Zagreb index" of* G *denoted by* $RM_2(G)$ *is given by*

$$RM_2(G) = n(mn - n + 3).$$

Proof. The proof is similar to the proof of Theorem 3.1. □

Theorem 3.4. *Let* $G = C_{m,n}$. *The "reverse arithmetic-geometric index" of* G *denoted by* $RAG(G)$ *is given by*

$$RAG(G) = \frac{1}{2}\left(2(m-3) + \frac{n(n+2)}{\sqrt{n+1}} + \frac{2n+1}{\sqrt{n(n+1)}} + \frac{n+1}{\sqrt{n}}\right).$$

Proof. We start by noting that the graph $G = C_{m,n}$ has $m-1+n$ edges with the following classification based on their end vertices: 1 leaf-internal edge, $m-3$ internal-internal edges, 1 internal-branching edge, and n branching-internal edges. Combining these information with equation (1) in Proposition 2.2 and the definition of the reverse arithmetic-geometric index, we arrive at

$$\begin{aligned} RAG(G) &= \sum_{uv \in E(G)} \frac{r_u + r_v}{2\sqrt{r_u \cdot r_v}} \\ &= \frac{(n+1)+n}{2\sqrt{(n+1)(n)}} + (m-3)\frac{n+n}{2\sqrt{(n)(n)}} + \frac{n+1}{2\sqrt{(n)(1)}} + (n)\frac{1+(n+1)}{2\sqrt{(1)(n+1)}} \\ &= \frac{1}{2}\left(2(m-3) + \frac{n(n+2)}{\sqrt{n+1}} + \frac{2n+1}{\sqrt{n(n+1)}} + \frac{n+1}{\sqrt{n}}\right). \end{aligned}$$

□

Theorem 3.5. *Let* $G = C_{m,n}$. *The "reverse geometric-arithmetic index" of* G *denoted by* $RGA(G)$ *is given by*

$$RGA(G) = (m-3) + \frac{2\sqrt{n}}{n+1} + \frac{2n\sqrt{n+1}}{n+2} + \frac{2\sqrt{n^2+n}}{2n+1}.$$

Proof. The proof is similar to the proof of Theorem 3.4. □

Theorem 3.6. *Let* $G = C_{m,n}$. *The "reverse Sombor index" of* G *denoted by* $RSO(G)$ *is given by*

$$RSO(G) = \sqrt{2}(m-3)n + \sqrt{n^2+1} + \sqrt{n^2+(n+1)^2} + n\sqrt{(n+1)^2+1}.$$

Proof. As with the previous proofs, we start with the fact that the graph $G = C_{m,n}$ has $m-1+n$ edges with the following classification based on their end vertices: 1 leaf-internal edge, $m-3$ internal-internal edges, 1 internal-branching edge, and n branching-internal edges. Combining these information with equation (1) in Proposition 2.2 and the definition of the reverse Sombor index, we arrive at

$$\begin{aligned} RSO(G) &= \sum_{uv\in E(G)} \sqrt{r_u^2+r_v^2} \\ &= \sqrt{(n+1)^2+n^2}+(m-3)\sqrt{n^2+n^2}+\sqrt{n^2+1^2}+n\sqrt{1^2+(n+1)^2} \\ &= \sqrt{2}(m-3)n+\sqrt{n^2+1}+\sqrt{n^2+(n+1)^2}+n\sqrt{(n+1)^2+1}. \end{aligned}$$

□

Theorem 3.7. *Let G =*$C_{m,n}$. *The "reverse Nirmala index" of G denoted by RN(G) is given by*

$$RN(G)=\sqrt{2n+1}+(m-3)\sqrt{2n}+\sqrt{n+1}+n\sqrt{n+2}.$$

Proof. The proof is similar to the proof of Theorem 3.6. □

3.2. Results for Double Comet Graphs

Next, we present our results for double comet graphs. Throughout this subsection, we denote the double comet graph $DC(m,m_1,m_2)$ by G, the maximum of $\{m_1,m_2\}$ by M, and the minimum of $\{m_1,m_2\}$ by μ.

Theorem 3.8. *Let* $G = DC(m,m_1,m_2)$. *Denote by* $M = max\{m_1,m_2\}$ *and* $\mu = min\{m_1,m_2\}$. *The "reverse sum-connectivity index" of G denoted by RSCI(G) is given by*

$$RSCI(G)=\frac{\mu}{\sqrt{2M+2-\mu}}+\frac{1}{\sqrt{2M+1-\mu}}+\frac{m-3}{\sqrt{2M}}+\frac{1}{\sqrt{M+1}}+\frac{M}{\sqrt{M+2}}.$$

Proof. For the proof of this result, we refer the readers to the proof provided in Theorem 3.10, since they are similar in nature. □

Theorem 3.9. *Let* $G = DC(m,m_1,m_2)$. *Denote by* $M = max\{m_1,m_2\}$ *and* $\mu = min\{m_1,m_2\}$. *The "first reverse Zagreb index" of G denoted by* $RM_1(G)$ *is given by*

$$RM_1(G)=(M+\mu)(M+1)^2+(m-2)M^2+(M-\mu+1)^2+1.$$

Proof. We start by noting that the graph $G = DC(m,m_1,m_2)$ has $m + m_1 + m_2 = m + \mu + M$ vertices with the following classification: $m_1 + m_2 = \mu + M$ leaf vertices, $m-2$ internal vertices, 1 branching vertex of degree $\mu+1$, and 1 branching vertex of degree $M+1$. Combining these information with equation (2) in Proposition 2.3 and the definition of the first reverse Zagreb index, we arrive at

$$\begin{aligned} RM_1(G) &= \sum_{u\in V(G)} r_u^2 \\ &= (M+\mu)(M+1)^2+(m-2)M^2+(M-\mu+1)^2+1^2 \\ &= (M+\mu)(M+1)^2+(m-2)M^2+(M-\mu+1)^2+1. \end{aligned}$$ □

Theorem 3.10. *Let* $G = DC(m,m_1,m_2)$. *Denote by* $M = max\{m_1,m_2\}$ *and* $\mu = min\{m_1,m_2\}$. *The"second reverse Zagreb index" of G denoted by* $RM_2(G)$ *is given by*

$$RM_2(G)=\mu(M+1)(M-\mu+1)+(m-3)M^2+(2M-\mu+3)M.$$

Proof. We start by noting that the graph $G = DC(m,m_1,m_2)$ has $(m-1) + m_1 + m_2 = (m-1)+\mu+M$ edges with the following classification based on their end vertices: $\mu+M$ leaf-branching (branching-leaf) edge, 2 internal-branching (branching-internal) edge, and $m-3$ internal-internal edges. Before we proceed, we emphasize that in the $\mu+M$ leaf-branching (branching-leaf) edge type, there are μ number of edges whose one end is the vertex with degree $\mu+1$ and M number of edges whose one end is the vertex with degree $M+1$. Also in the 2 internal-branching (branching-internal) edge type, 1 edge has the vertex of degree μ +1 as one end vertex, while the other edge has the vertex of degree M +1 as one end vertex. Combining these information with equation (2) in Proposition 2.3 and the definition of the second reverse Zagreb index, we arrive at

$$\begin{aligned} RM_2(G) &= \sum_{uv\in E(G)} (r_u \cdot r_v) \\ &= \mu\left((M+1)(M-\mu+1)\right) + (M-\mu+1)(M) + (m-3)\left((M)(M)\right) + (M)(1) \\ &+ M\left((1)(M+1)\right) \\ &= \mu(M+1)(M-\mu+1) + (m-3)M^2 + (2M-\mu+3)M. \end{aligned}$$

□

Theorem 3.11. *Let G = DC(m,m_1,m_2). Denote by M = max{m_1,m_2} and μ = min{m_1,m_2}. The "reverse arithmetic-geometric index" of G denoted by RAG(G) is given by*

$$RAG(G) = \mu\left(\frac{2M+2-\mu}{2\sqrt{(M+1)(M-\mu+1)}}\right) + \frac{2M+1-\mu}{2\sqrt{(M-\mu+1)M}} + (m-3) + \frac{M+1}{2\sqrt{M}} + M\left(\frac{M+2}{2\sqrt{M+1}}\right).$$

Proof. The proof is similar to the proof provided in Theorem 3.12. □

Theorem 3.12. *Let G = DC(m,m_1,m_2). Denote by M = max{m_1,m_2} and μ = min{m_1,m_2}. The "reverse geometric-arithmetic index" of G denoted by RGA(G) is given by*

$$RGA(G) = \mu\left(\frac{2\sqrt{(M+1)(M-\mu+1)}}{2M+2-\mu}\right) + \frac{2\sqrt{(M-\mu+1)M}}{2M+1-\mu} + (m-3) + \frac{2\sqrt{M}}{M+1} + M\left(\frac{2\sqrt{M+1}}{M+2}\right).$$

Proof. Similar to what we did earlier, we start by noting that the graph $G = DC(m, m_1, m_2)$ has $(m-1) + m_1 + m_2 = (m-1) + \mu + M$ edges with the following classification based on their end vertices: $\mu+M$ leaf-branching (branching-leaf) edge, 2 internal-branching (branching-internal) edge, and $m-3$ internal-internal edges. Again, we emphasize that in the $\mu + M$ leaf-branching (branching-leaf) edge type, there are μ number of edges whose one end is the vertex with degree μ +1 and M number of edges whose one end is the vertex with degree M +1. Also in the 2 internal-branching (branching-internal) edge type, 1 edge has the vertex of degree μ + 1 as one end vertex, while the other edge has the vertex of degree M +1 as one end vertex. Combining these information with equation (2) in Proposition 2.3 and the definition of the reverse geometric-arithmetic index, we arrive at

$$\begin{aligned} RGA(G) &= \sum_{uv\in E(G)} \frac{2\sqrt{r_u \cdot r_v}}{r_u + r_v} \\ &= \mu\left(\frac{2\sqrt{(M+1)(M-\mu+1)}}{(M+1)+(M-\mu+1)}\right) + \frac{2\sqrt{(M-\mu+1)(M)}}{(M-\mu+1)+M} + (m-3)\left(\frac{2\sqrt{(M)(M)}}{M+M}\right) \\ &+ \frac{2\sqrt{(M)(1)}}{M+1} + M\left(\frac{2\sqrt{(1)(M+1)}}{1+(M+1)}\right). \end{aligned}$$

Simplifying the above displayed equation will give us

$$RGA(G) = \mu\left(\frac{2\sqrt{(M+1)(M-\mu+1)}}{2M+2-\mu}\right) + \frac{2\sqrt{(M-\mu+1)M}}{2M+1-\mu} + (m-3) + \frac{2\sqrt{M}}{M+1} + M\left(\frac{2\sqrt{M+1}}{M+2}\right).$$

This proves the theorem. □

Theorem 3.13. *Let $G = DC(m,m_1,m_2)$. Denote by $M = max\{m_1,m_2\}$ and $\mu = min\{m_1,m_2\}$. The "reverse Sombor index" of G denoted by $RSO(G)$ is given by*

$$RSO(G) = \mu\left(\sqrt{(M+1)^2+(M-\mu+1)^2}\right)+\sqrt{(M-\mu+1)^2+M^2}+\sqrt{2}(m-3)M+\sqrt{M^2+1} + M\left(\sqrt{M^2+2M+2}\right).$$

Proof. The proof of this theorem is similar to the proof of Theorem 3.14. □

Theorem 3.14. *Let $G = DC(m,m_1,m_2)$. Denote by $M = max\{m_1,m_2\}$ and $\mu = min\{m_1,m_2\}$. The "reverse Nirmala index" of G denoted by $RN(G)$ is given by*

$$RN(G) = \mu\sqrt{2M+2-\mu}+\sqrt{2M+1-\mu}+(m-3)\sqrt{2M}+\sqrt{M+1}+M\sqrt{M+2}.$$

Proof. Again, we start by noting that the graph $G = DC(m,m_1,m_2)$ has $(m-1) + m_1 + m_2 = (m-1) + \mu + M$ edges with the following classification based on their end vertices: $\mu + M$ leaf-branching (branching-leaf) edge, 2 internal-branching (branching-internal) edge, and $m-3$ internal-internal edges. Moreover, we emphasize that in the $\mu+M$ leaf-branching (branching-leaf) edge type, there are μ number of edges whose one end is the vertex with degree $\mu+1$ and M number of edges whose one end is the vertex with degree $M+1$. Also in the 2 internal-branching (branching-internal) edge type, 1 edge has the vertex of degree $\mu+1$ as one end vertex, while the other edge has the vertex of degree $M+1$ as one end vertex. Combining these information with equation (2) in Proposition 2.3 and the definition of the reverse Nirmala index, we arrive at

$$\begin{aligned} RN(G) &= \sum_{uv\in E(G)} \sqrt{r_u+r_v} \\ &= \mu\sqrt{(M+1)+(M-\mu+1)}+\sqrt{(M-\mu+1)+M}+(m-3)\sqrt{M+M} \\ &+\sqrt{M+1}+M\sqrt{1+(M+1)} \\ &= \mu\sqrt{2M+2-\mu}+\sqrt{2M+1-\mu}+(m-3)\sqrt{2M}+\sqrt{M+1}+M\sqrt{M+2}. \end{aligned}$$

□

3.3 Reverse Vertex Degree Indices of 2,2,4,4-Tetramethylpentane

For this subsection, we illustrate a particular computational application of Theorems 3.8 - 3.14 obtained in the previous section. Observe that the molecule 2,2,4,4-Tetramethylpentane in the introductory section has $DC(3,3,3)$ as a molecular graph. Hence, we have the following immediate results.

Corollary 3.15. *Let G denote the molecular graph of 2,2,4,4-Tetramethylpentane, then*

(i) $RSCI(G) = \frac{5+6\sqrt{5}}{5}$,

(ii) $RM_1(G) = 107$,

(iii) $RM_2(G) = 30$,

(iv) $RAG(G) = \frac{45+8\sqrt{3}}{6}$,

(v) $RGA(G) = \frac{24+5\sqrt{3}}{5}$,

(vi) $RSO(G) = 6\sqrt{17}+2\sqrt{10}$,

(vii) $RN(G) = 4+6\sqrt{5}$.

3.4 Relationship Between the Results for Bistar and for Double Comet

This subsection investigates the relationship between the reverse vertex degree-based topological indices of bistars and double comets. The motivation for this subsection is the fact that the bistar $B(m_1, m_2)$ is the double comet $DC(2\ m_1, m_2)$. Hence, we can obtain $DC(m, m_1, m_2)$ from $DC(2, m_1, m_2)$ by expanding P_2 to P_m. Specifically, by adding vertices and edges to P_2 to become P_m. The results in this subsection are obtained by calculating the difference between a particular reverse topological index of the double comet and bistar. For instance, if the concerned topological index is RM_1, then we calculate $RM_1(DC(m,m_1,m_2))-RM_1(B(m_1,m_2))$. The computation is of course based on the results of Gowtham and Husin summarized in subsection 2.1, and the results of this paper provided in subsection 3.2.

Theorem 3.16. *Let $G_1 = DC(m,m_1,m_2)$ and $G_2 = B(m_1,m_2)$. If $M = max\{m_1,m_2\}$ and $\mu = min\{m_1,m_2\}$, then*

$$RSCI(G_1) - RSCI(G_2) = \frac{1}{\sqrt{2M+1-\mu}} + \frac{m-3}{\sqrt{2M}} + \frac{1}{\sqrt{M+1}} - \frac{1}{\sqrt{M+2-\mu}}.$$

Theorem 3.17. *Let $G_1 = DC(m,m_1,m_2)$ and $G_2 = B(m_1,m_2)$. If $M = max\{m_1,m_2\}$ and $\mu = min\{m_1,m_2\}$, then*

$$RM_1(G_1) - RM_1(G_2) = (m-2)M^2.$$

Theorem 3.18. *Let $G_1 = DC(m,m_1,m_2)$ and $G_2 = B(m_1,m_2)$. If $M = max\{m_1,m_2\}$ and $\mu = min\{m_1,m_2\}$, then*

$$RM_2(G_1) - RM_2(G_2) = mM^2 + 2M - M^2 - 2\mu M - 1.$$

Theorem 3.19. *Let $G_1 = DC(m,m_1,m_2)$ and $G_2 = B(m_1,m_2)$. If $M = max\{m_1,m_2\}$ and $\mu = min\{m_1,m_2\}$, then*

$$RAG(G_1) - RAG(G_2) = \frac{2M+1-\mu}{2\sqrt{(M-\mu+1)(M)}} + (m-3) + \frac{M+1}{2\sqrt{M}} - \frac{M-\mu+2}{2\sqrt{M-\mu+1}}.$$

Theorem 3.20. *Let $G_1 = DC(m,m_1,m_2)$ and $G_2 = B(m_1,m_2)$. If $M = max\{m_1,m_2\}$ and $\mu = min\{m_1,m_2\}$, then*

$$RGA(G_1) - RGA(G_2) = \frac{2\sqrt{(M-\mu+1)(M)}}{2M+1-\mu} + (m-3) + \frac{2\sqrt{M}}{M+1} - \frac{2\sqrt{M-\mu+1}}{M-\mu+2}.$$

Theorem 3.21. *Let $G_1 = DC(m,m_1,m_2)$ and $G_2 = B(m_1,m_2)$. If $M = max\{m_1,m_2\}$ and $\mu = min\{m_1,m_2\}$, then*

$$RSO(G_1) - RSO(G_2) = \sqrt{(M-\mu+1)^2 + M^2} + \sqrt{2}(m-3)M + \sqrt{M^2+1} - \sqrt{(M-\mu+1)^2+1}.$$

Theorem 3.22. *Let $G_1 = DC(m,m_1,m_2)$ and $G_2 = B(m_1,m_2)$. If $M = max\{m_1,m_2\}$ and $\mu = min\{m_1,m_2\}$, then*

$$RN(G_1) - RN(G_2) = \sqrt{2M+1-\mu} + (m-3)\sqrt{2M} + \sqrt{M+1} - \sqrt{M-\mu+2}.$$

4. Conclusion and Future Work

In this paper, the results obtained in Theorem 3.1 - Theorem 3.7 show that we were able to compute for the Reverse sum-connectivity ($RSCI(\cdot)$), First reverse Zagreb ($RM_1(\cdot)$), Second reverse Zagreb

($RM_2(\cdot)$), Reverse arithmetic-geometric ($RAG(\cdot)$), Reverse geometric-arithmetic ($RGA(\cdot)$), Reverse Sombor ($RSO(\cdot)$), and Reverse Nirmala ($RN(\cdot)$) of comet graphs. The same reverse vertex degree-based topological indices were calculated for double comet graphs and were presented in Theorem 3.8 - Theorem 3.14. We also have presented a computational application of our results to a specific molecule. Lastly, we have determined the relationship between various reverse vertex degree-based topological indices of bistar and double comet graphs as presented in Theorem 3.16 - Theorem 3.22.

For future studies, we recommend the study of the determination of reverse vertex degree-based topological indices for other families of trees.

5. Acknowledgements

The authors would like to thank the anonymous reviewers for their comments and suggestions that helped improve the overall content of the paper. Special thanks to the Central Luzon State University and its administration for their motivation and support throughout the conduct and publication of this study.

References

[1] Compound summary 2,2,4,4-tetramethylpentane. https://pubchem.ncbi.nlm.nih.gov/ compound/2_2_4_4-Tetramethylpentane. Accessed: 2024-03-25.

[2] A. Ahmad, A. N. Koam, and M. Azeem. Reverse-degree-based topological indices of fullerene cage networks. *Molecular Physics*, 121(14): e2212533, 2023.

[3] W. Ahmed, K. Ali, S. Zaman, and A. Raza. Molecular insights into anti-alzheimers drugs through predictive modeling using linear regression and qspr analysis. *Modern Physics Letters B*, page 2450260, 2024.

[4] M. Al-Sharafi and A. Alameri. Computation of wiener polynomial and index of line subdivision friendship and line subdivision bifriendship graphs using matlab program. *Proyecciones (Antofagasta, On line)*, 43(1), 2024.

[5] U. Ali, J. Li, Y. Ahmad, and Z. Raza. Computing the laplacian spectrum and wiener index of pentagonal-derivation cylinder/mobius network.¨ *Heliyon*, 10(2), 2024.

[6] J. ANTALAN and F. CAMPENA. Distance eigenvalues, forwarding indices, and distance-based˜ topological indices of complement of two circulant networks. *TWMS Journal of Applied & Engineering Mathematics*, 13(3), 2023.

[7] J. R. M. Antalan, F. J. H. Campena, and E. D. Iba˜ nez. A note on some distance-based topo-˜ logical indices of circulant network cn (1, a). *Journal of Discrete Mathematical Sciences and Cryptography*, 25(1):107–125, 2022.

[8] S. A. U. H. Bokhary, P. Bashir, A. Nawaz, S. O. Hilali, M. Alhagyan, A. Gargouri, M. Almazah, et al. Computation of wiener and wiener polarity indices of a class of nanostar dendrimer using vertex weighted graphs. *Journal of Mathematics*, 2024, 2024.

[9] A. A. Dobrynin and K. V. Vorobev. Some results on the wiener index related to the soltˇ es problem´ of graphs. *Discrete Applied Mathematics*, 344:154–160, 2024.

[10] D. D. Durgun and E. N. Toprakkaya. Roman domination of the comet, double comet, and comb graphs. *arXiv preprint arXiv:2102.07902*, 2021.

[11] M. C. G. Egan, J. R. M. Antalan, et al. On the wiener and harary index of splitting graphs. *European Journal of Pure and Applied Mathematics*, 15(2):602–619, 2022.

[12] K. Gowtham and M. Husin. A study of families of bistar and corona product of graph: Reverse topological indices. *Malaysian Journal of Mathematical Sciences*, 17(4), 2023.

[13] I. Gutman and N. Trinajstic. Graph theory and molecular orbitals. total´ ϕ-electron energy of alternant hydrocarbons. *Chemical physics letters*, 17(4):535–538, 1972.

[14] M. Hasani and M. Ghods. Calculation of topological indices along with matlab coding in qspr analysis of calcium channel-blocking cardiac drugs. *Journal of Mathematical Chemistry*, pages 1–22, 2024.

[15] M. Hasani and M. Ghods. Topological indices and qspr analysis of some chemical structures applied for the treatment of heart patients. *International Journal of Quantum Chemistry*, 124(1):e27234, 2024.

[16] R. Huang, A. Mahboob, M. W. Rasheed, S. M. Alam, and M. K. Siddiqui. On molecular modeling and qspr analysis of lyme disease medicines via topological indices. *The European Physical Journal Plus*, 138(3):243, 2023.

[17] S. A. K. Kirmani, P. Ali, and F. Azam. Topological indices and qspr/qsar analysis of some antiviral drugs being investigated for the treatment of covid-19 patients. *International Journal of Quantum Chemistry*, 121(9):e26594, 2021.

[18] V. Kulli. Reverse zagreb and reverse hyper-zagreb indices and their polynomials of rhombus silicate networks. *Annals of Pure and Applied Mathematics*, 16(1):47–51, 2018.

[19] Y. C. Kwun, A. U. R. Virk, M. Rafaqat, M. U. Rehman, and W. Nazeer. Some reversed degreebased topological indices for graphene. *Journal of Discrete Mathematical Sciences and Cryptography*, 22(7):1305–1314, 2019.
[20] L. Li, X. Li, and W. Liu. Note on the product of wiener and harary indices. *MATCH Commun. Math. Comput. Chem*, 91:299–305, 2024.
[21] Z. Li and B. Wu. Orientations of graphs with maximum wiener index. *Journal of Graph Theory*.
[22] Y. Liu, M. Rezaei, M. R. Farahani, M. N. Husin, and M. Imran. The omega polynomial and the cluj-ilmenau index of an infinite class of the titania nanotubes tio2 (m, n). *Journal of Computational and Theoretical Nanoscience*, 14(7):3429–3432, 2017.
[23] A. Mahboob, M. W. Rasheed, A. M. Dhiaa, I. Hanif, and L. Amin. On quantitative structureproperty relationship (qspr) analysis of physicochemical properties and anti-hepatitis prescription drugs using a linear regression model. *Heliyon*, 2024.
[24] A. Mahboob, M. W. Rasheed, I. Hanif, L. Amin, and A. Alameri. Role of molecular descriptors in quantitative structure-property relationship analysis of kidney cancer therapeutics. *International Journal of Quantum Chemistry*, 124(1):e27241, 2024.
[25] M. Randic. Characterization of molecular branching. *Journal of the American Chemical Society*, 97(23):6609–6615, 1975.
[26] M. S. Rosary. On reverse valency based topological indices of metal–organic framework. *Polycyclic Aromatic Compounds*, 43(1):860–873, 2023.
[27] S. Wagner and H. Wang. *Introduction to Chemical Graph Theory*. CRC Press, Taylor & Francis Group, Boca Raton, FL, 2018.
[28] J. Wei, A. Khalid, P. Ali, M. K. Siddiqui, A. Nawaz, and M. Hussain. Computing reverse degree based topological indices of vanadium carbide. *Polycyclic Aromatic Compounds*, 43(2):1172– 1191, 2023.
[29] H. Wiener. Correlation of heats of isomerization, and differences in heats of vaporization of isomers. *Journal of American Chemical Society*, 69:2636–2638, 1947.
[30] S. Zaman, H. S. A. Yaqoob, A. Ullah, and M. Sheikh. Qspr analysis of some novel drugs used in blood cancer treatment via degree based topological indices and regression models. *Polycyclic Aromatic Compounds*, pages 1–17, 2023.
[31] S. Zhang, X. Chen, Z.-W. Ma, X.-D. Zhang, and Y.-H. Chen. The minimum wiener index of unicyclic graphs with maximum degree. *Applied Mathematics and Computation*, 470:128581, 2024.
[32] X. Zhang, A. Rauf, M. Ishtiaq, M. K. Siddiqui, and M. H. Muhammad. On degree based topological properties of two carbon nanotubes. *Polycyclic Aromatic Compounds*, 42(3):866–884, 2022.
[33] X. Zhang, H. Reddy, A. Usha, M. Shanmukha, M. Reza Farahani, and M. Alaeiyan. A study on anti-malaria drugs using degree-based topological indices through qspr analysis. 2022.
[34] X. Zhang, M. K. Siddiqui, S. Javed, L. Sherin, F. Kausar, and M. H. Muhammad. Physical analysis of heat for formation and entropy of ceria oxide using topological indices. *Combinatorial Chemistry & High Throughput Screening*, 25(3):441–450, 2022.
[35] H. Zhou, A. Mahboob, M. W. Rasheed, A. Ovais, M. K. Siddiqui, and I. Z. Cheema. On qspr analysis of molecular descriptor and thermodynamic features of narcotic drugs. *Polycyclic Aromatic Compounds*, pages 1–21, 2023.
[36] X. Zuo, J.-B. Liu, H. Iqbal, K. Ali, and S. T. R. Rizvi. Topological indices of certain transformed chemical structures. *Journal of Chemistry*, 2020:1–7, 2020.